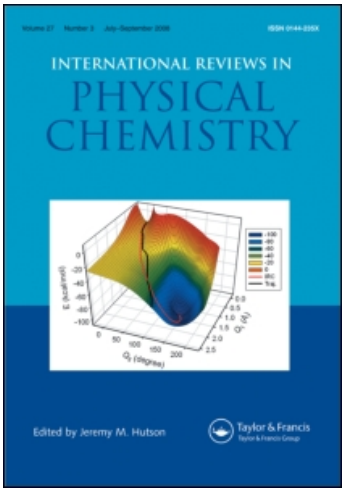

International Reviews in Physical Chemistry
Publication details, including instructions for authors and subscription information:
http://www.informaworld.com/smpp/title~content=t713724383

Low-temperature rate studies of ions and radicals in supersonic flows

Mark A. Smith

Online publication date: 26 November 2010

To cite this Article Smith, Mark A.(1998) 'Low-temperature rate studies of ions and radicals in supersonic flows', International Reviews in Physical Chemistry, 17: 1, 35 — 63
To link to this Article: DOI: 10.1080/014423598230162
URL: http://dx.doi.org/10.1080/014423598230162

INTERNATIONAL REVIEWS IN PHYSICAL CHEMISTRY, 1998, VOL. 17, NO. 1, 35–63

Low-temperature rate studies of ions and radicals in supersonic flows

by MARK A. SMITH

Department of Chemistry, University of Arizona, Tucson, AZ 85721, USA

Studies of the rates of gas-phase ion–molecule and neutral chemistry at low temperatures using supersonic flow methods are reviewed. The current supersonic flow methods employed are discussed, together with the experimental and theoretical models utilized for their full understanding. Particular emphasis in the review is placed upon recent investigations into chemical reaction as well as inelastic energy transfer processes which display a high efficiency at the low temperatures. These studies have particular relevance to the development of broadly applicable reaction dynamic models at the quantum state specific level. The results are assisting the growing understanding of natural chemical environments at very low temperatures such as planetary atmospheres, cometary gases and interstellar molecular clouds. Future directions of the young field of low-temperature gas kinetics are discussed.

Contents

1. Introduction

In the past 25 years we have seen a tremendous growth in both experimental and theoretical developments in the area of gas-phase chemistry and collision dynamics [1, 2]. The growth in theoretical understanding stems from advancements allowed by the practical developments in high-speed computation that have permitted sophisticated and highly accurate numerical methods in scattering dynamics to be implemented.

0144–235X/98 $12.00

Much of this work has been fuelled by the rich diversity in experimental information coming from detailed studies of inelastic and reactive cross-sections over a wide range of energies. These include both integral and differential scattering cross-sections as well as state-specific cross-sections and rate coefficients. The combined studies have begun to yield, for the first time, highly accurate knowledge of the potential energy surfaces for collisions of moderately complex systems.

These developments have reconciled many mysteries in the area of thermal and hyperthermal reactions, the energy regimes that encompassed nearly all chemical information prior to 1985. During this same time, however, there has been growing interest in the chemistry of very-low-temperature environments such as exist in planetary atmospheres, comets and the interstellar medium. As a result, during the past decade we have seen a variety of novel developments in experimental methodology that have opened up the energy window below 200 K to general kinetic investigations [3–5]. It has now become possible to make direct laboratory investigations into many of the general processes proposed to dominate the chemistry of such environments. These studies have stimulated new developments in the theory of chemical reaction processes in the limit of very low energy and the models of these environments have begun to undergo rapid development.

One striking example of the result of this growth is in the area of chemical dynamics in low-temperature interstellar clouds. Owing to the large fractional ionization in these media and typical temperatures in the range of 50 K, the early chemical models were almost exclusively dominated by ion–molecule reactions [6–10]. This well founded bias stems from the long-standing knowledge that the vast majority of exoergic ion–molecule reaction systems are observed to proceed at nearly gas kinetic rates and show little or no temperature dependence near 300 K. When ion–molecule reactions do show a temperature dependence, it is usually inverse in nature, the reaction rate increasing with decreasing temperature, and is largely attributable to simple electrostatic forces between the colliding species. As a result, coupled ion–molecule reactions, photoionization events and ion–electron recombination cycles form an ideal system for generating complex molecular environments at the extreme low temperatures of interstellar space.

The more recent observation that many neutral–neutral reaction systems display striking and many times unanticipated inverse temperature dependences has led to a rapid re-evaluation of the alternative schemes for molecular synthesis in extreme low-temperature environments [11–15]. Many of our perceptions of molecule kinetics largely derive from high-temperature studies. It has now become very clear that these give only a partial description of the true and complex dynamics applicable to reacting systems. Their use to extrapolate behaviour to extreme conditions should be done with great caution.

The rich field of low-temperature kinetics has focused on ion–molecule as well as neutral chemistry, and surprising results have been found in both types of system. The low-energy experimental methods employed for the ion studies have included low-temperature drift studies, a variety of trapping techniques, free jet flow methods and axisymmetric supersonic flow methods [3]. These methods and their successes have been the subject of a recent review. The group of Dieter Gerlich, in Chemnitz, is at present studying low-temperature ion collisions in cryogenically cooled radio-frequency ion traps, and Gerlich [16] has produced a superb review of this technology. The group of Bertrand Rowe, in Rennes, has developed a variety of axisymmetric supersonic flow techniques employing Laval nozzles [4, 17]. Our group, in Tucson, has

focused on the use of collisions in rarified supersonic free jet flows for ion–molecule reaction studies [18]. In the area of low-temperature neutral collisions, the majority of results derive from three groups and are all predominantly centred on the use of Laval nozzle flows. These are the groups in Rennes [4] and Tucson [5] as well as the group of Ian Smith in Birmingham [11]. Our group has also recently begun to explore the use of free jets to investigate neutral reactions very near the 0 K limit. What is very clear, however, is that this remains a very young field which is exploring highly uncharted territory with only a limited range of techniques. It is to be hoped that this review will stimulate ideas and interest in exploring new and innovative methods to confirm further some of the exciting results which are emerging and hopefully open new vistas for investigation.

This review will focus upon recent studies of a variety of low-temperature processes studied in our laboratory using both free jet and Laval nozzle supersonic flow methods. Particular emphasis is placed upon inelastic and reactive processes which display prominent inverse temperature dependence in the low-temperature limit, behaviour that is not indicated in the majority of previous studies with conventional methods at temperatures above 200 K. This review is not meant to be exhaustive. The intention is more to provide the reader with a broad view of the types of process amenable to low-temperature study and a few of the surprising results which have emerged. From the references cited, it should then be possible to trace the entire low-temperature kinetics field in more detail should a complete review be desired.

2. Experimental methods

2.1. *Free jet supersonic flows*

Free jet flows have provided a viable very-low-temperature collision environment for the study of a wide range of inelastic and reactive processes. Our use of free jet flows as a viable medium for the study of ion–molecule interactions at temperatures below 20 K has been well documented in several reviews [18, 19]. Free jet expansions employ isentropic expansion to effect cooling. The expansion remains everywhere unrestricted by nozzle walls, resulting in a flow that evolves to high Mach numbers and therefore very low local temperatures approaching 1 K [20]. There are several advantages to the use of free jet flows for low-temperature kinetic studies. The first is the extremely simple design of the nozzle. The ideal free expansion is one where the gas expands through a small-diameter orifice of infinite thinness, into a chamber of much lower density. The mean free path of the gas backing the nozzle must be much less than the nozzle diameter. Given a sufficiently large gradient in this mean free path near the nozzle exit, one gets stable adiabatic expansion. The high collision rate near the nozzle exit tends to smooth out the effects of nozzle thickness and surface imperfections in these flows. The small dimensions, with nozzle diameters typically ranging between 0.1 and 1 mm, have allowed development of a short-duration pulsed valve source which, together with the small size scale, dramatically cut down on gas consumption and pumping requirements. With standard equipment, it is possible to produce kinetically well defined jets down to 300 μs duration. Pulsing these jets at 10 Hz, with stagnation pressures below 1 atm, consumes relatively small quantities of gas of the order of 10 SCCM.

Using high-powered pulsed dye lasers which operate at these same repetition frequencies, such a source is ideal for laser ionization as a means of ion production. By expanding a mixture of buffer gas, ion precursor and reactant neutral, a low-temperature gas at constant flow velocity is obtained within ten to 30 nozzle diameters

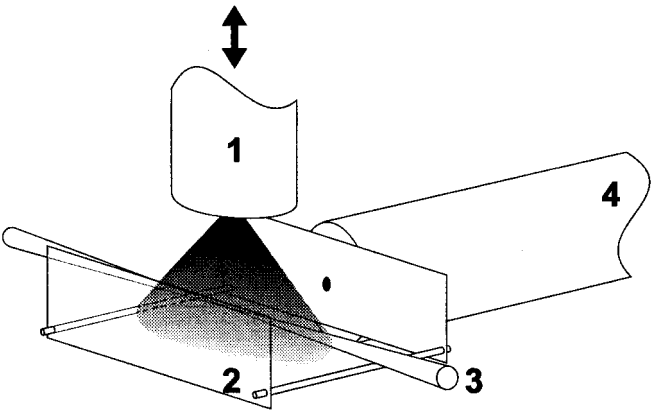

Figure 1. A schematic diagram of the interaction zone of the free jet flow apparatus of Smith and co-workers. Free jet flows are initiated via a pulsed beam valve 1, with subsequent reaction initiation using selective resonance-enhanced multiphoton ionization (REMPI) from the focused pulsed-laser source. The ions are later pulse extracted via a temporal voltage on the repeller plate 2 and directed to the grounded entrance plate 3 of a time-of-flight mass spectrometer 4. The mass analyser is capable of monitoring the laser-prepared ion packet for reaction times in excess of 300 μs via translation down the centre flow streamline of the jet.

downstream of the nozzle exit plane. As depicted in figure 1, one can then cross this jet with the focused output of a pulsed dye laser tuned to a multiphoton absorption resonance in the cooled precursor species. Absorption followed by rapid photo-ionization of the selectively prepared excited state then produces a well defined parent radical cation of the precursor without disturbing any other feature of the flow. Judicious selection of precursor and intermediate resonant state has allowed production of atomic and molecular cations in well defined internal quantum states. Although most studies have been aimed at production of cold ground-state ions, in others it has been possible to study collisional processes in the vibrationally excited molecular ions, such as NO^+ ($v = 1$) and $C_2H_2^+(\nu_3 = 1)$, as well as electronically excited atomic ions, for instance the hyperfine excited state $Ar^+(^2P_{1/2})$ or $Xe^+(^2P_{1/2})$. At sufficiently low laser powers, the ionization does not affect the temperature distribution of the ions. In this way, the laser ionization free jet source produces a clean single-ion packet of charged species in the core of a cold jet containing reactive neutrals. The results of subsequent ion–molecule reactive collisions can be monitored by extraction of the ion packet at various distances downstream of ionization. Mass analysis is accomplished most efficiently via time-of-flight mass spectrometry.

Although there are several advantages to using a laser ionization free jet flow technique, there are also some complications unique to this method. All these complexities are a result of the fact that the flow continues to expand at all positions following the nozzle exit. The most obvious consequence is that the changing density results in a continuously dropping collision rate in the jet and this must be accounted for in the data work-up. Fortunately, after a few nozzle diameters of flow, the gas expansion rate becomes a constant which is easily accounted for in the integrated rate expressions. A more difficult consequence of the expansion concerns the disequilibria which develops in temperature with distance. Although this cooling is quite a complicated process, it has been shown that in most cases it remains possible to assign

a well defined average temperature to the collisions in the jet core [18, 21]. Thorough analysis of cooling in atomic, molecular and mixed free jet expansions has now been made [20, 22–24]. By performing reaction studies in regions of flow where the neutral–neutral collision rate is negligible, the mean ion–molecule collision temperature becomes nearly constant across the distance of measurement.

Although the disequilibria in jets can be problematic for certain studies, one great benefit of working with a jet is the uniquely low temperatures that may be obtained. Thus, through variation in stagnation conditions and buffer gases, it is possible to study chemical reaction rates in temperatures between 20 and 0.1 K.

2.2. *Axisymmetric supersonic laval flows*

The extensive cooling effected by supersonic expansions has been widely exploited for the study of atomic and molecular properties. The free jet is pervasive in modern spectroscopic and dynamical applications, particularly in the study of weakly bound molecules; yet in many cases the densities and thermal distributions are less than ideal. In spite of these difficulties, the inherent simplicity of production of free jets has made them relatively commonplace in the physical laboratory. Among the potential drawbacks of free jets are that the accessible temperature range is generally restricted to below 20 K and the number density is typically less than 10^{15} molecules cm^{-3} in most of the usable areas of the jet. Additionally, the rotational distribution has been demonstrated to have a non-equilibrium nature [25, 26] although this does not impact significantly on most studies. More importantly for dynamical applications, the nature of the spherical expansion forces strong anisotropies in the velocity, temperature and density moments of the resulting flow [23]. The different temperature moments (translation, rotation and vibration) are not in equilibrium in the region of the jet typically employed in laboratory studies, and the effects of velocity and temperature slip need to be considered when atoms or molecules are seeded into a free jet. Extensive use has been made of free jets in spectroscopy, where these non-equilibrium and anisotropic aspects of the flow are not an issue. Uniform expansions can overcome some of the difficulties of free jets by maintaining local equilibrium at all points in the flow. While not without their own class of limitations, these flows can provide an alternative, if not at times more suitable, environment for a variety of applications.

The key to producing a uniform expansion is the Laval nozzle [5, 27]. This is an optimally shaped convergent divergent nozzle producing a flow at the exit which is at a constant Mach number, the consequence being that the density and temperature at all points within the subsequent post-nozzle flow are constant. It is then possible to continue the flow in this uniform manner following the nozzle exit for distances exceeding ten nozzle exit diameters. Another, perhaps more intuitive way of phrasing this is that there are no temperature or density gradients in the flow past the nozzle exit; local equilibrium has been established, and the flow moves at a constant velocity through the stagnant background gas.

The Laval nozzle was first developed a half-century ago for use in supersonic wind tunnels, where the design criteria for these applications was that a short length of uniform flow had to be produced with as great a cross-sectional area as possible. As has been pointed out, the design criteria for physical and chemical applications can be somewhat different [5]. For dynamical studies where temporal information is required, the cross-sectional area of the flow need not be very large but the axial length should be as long as possible.

The literature on the use of uniform supersonic flows for applications other than wind tunnels is somewhat sparse. Wegener [28] used the flow inside of a two-dimensional Laval nozzle to follow the kinetics of NO_2 dimerization in a N_2 flow, but this research was motivated primarily by a desire to study the effects of a chemical reaction on the flow properties of the nozzle, and no other reaction studies were subsequently reported. Marte *et al.* [29] at the Jet Propulsion Laboratory investigated the reaction of ozone with nitric oxide in a two-dimensional nozzle of less than ideal design, and again no further reaction studies have been reported. D'Amato and co-workers [30] have performed infrared absorption spectroscopy in a two-dimensional Laval nozzle, although problems of separating wall processes from ideal flow characteristics have been encountered. Several groups, including that of Stein [31], have used nozzles in cluster expansions, because of the very high centreline densities and thus collision frequencies which are produced. These nozzles were very small in diameter, causing their flows to be mostly non-ideal from the adiabatic standpoint and thus the uniformity of the expansion in the post-nozzle exit region was not good. As previously mentioned, Rowe and co-workers [4, 11] have very successfully studied the kinetics of a variety of ion–molecule reactions in the post-nozzle exit flow from an axisymmetric nozzle. More recently, the Rowe group, in collaboration with the Smith group in Birmingham, has begun to study radical–molecule reactions in the uniform flow produced by an axisymmetric Laval nozzle [17]. Finally, parallel efforts by our group have produced results on radical–radical association and radical–molecule reaction kinetics [5, 12, 32]. It is clear from these latter studies that axisymmetric flows provide an excellent medium for the study of molecular collision processes at low temperatures.

While free jets may be formed by simply expanding gas through a thin plate orifice into an appropriately evacuated chamber, the production of a uniform expansion is more involved. In this regard, an interactive computer program has been developed containing all the important flow methodology necessary to generate nozzle designs for target conditions, copies of which are available on request from the author. What is to be gained from this greater involvement is a rapidly produced, thermally equilibrated low-temperature environment, not necessarily at chemical equilibrium, which can be used to study molecular properties either at the local thermal condition or during the approach to chemical equilibrium. In particular, the desirable characteristics of the uniform expansion are that a 'plug flow' of fixed Mach number is formed with parallel streamlines. The Mach number is a useful dimensionless parameter for describing the flow of compressible fluids and is defined as the ratio of the hydrodynamic flow velocity to the local speed of sound. Thus it is essentially the ratio of flow speed to the rate of collisional information transfer in the flowing medium. In the travelling frame there is a well defined isotropic temperature which remains constant for the full length of the flow. The density and chemical composition of the flow also remain constant under non-reactive conditions. Since the density of these flows can be very high compared with those of free jets, the collision rate is high, and the degrees of freedom of the molecules making up the flow are more likely to remain in equilibrium; yet chemical equilibrium need not be established. Provided that the flow is accelerated to a uniform design Mach number M, the extent of cooling and density drop are well predicted by the one-dimensional relationships [33].

$$\frac{T}{T_0} = \left(1 + \frac{\gamma - 1}{2} M^2\right)^{-1}, \tag{1}$$

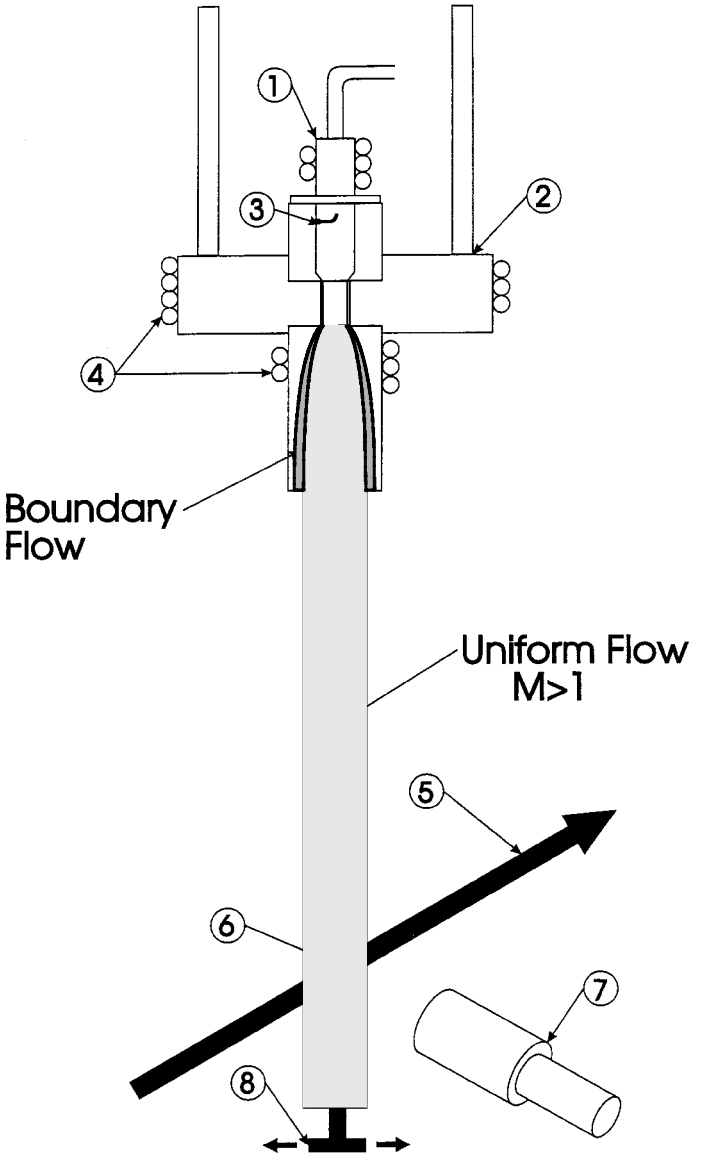

Figure 2. A diagram depicting the pulsed uniform Laval flow reactor used in our laboratory: 1, pulsed valve; 2, translation stage; 3, discharge source; 4, thermal coils; 5, laser-induced fluorescence (LIF) laser path; 6, fluorescence image; 7, LIF camera; 8, Pitot transducer.

$$\frac{\rho}{\rho_0} = \left(1 + \frac{\gamma - 1}{2} M^2\right)^{-1/(\gamma - 1)} \tag{2}$$

where T and ρ are the flow temperature and density respectively, T_0 and ρ_0 are the temperature and density respectively in the pre-expansion stagnation region, and γ is the ratio of the heat capacities, that is C_p/C_V.

The first part of the nozzle, as depicted for our instrument in Figure 2, is a short convergent section where the flow begins to accelerate from near-zero net hydrodynamic velocity in the stagnation region. Following this is a throat region where the diameter of the nozzle is at a minimum; at this point the flow reaches Mach 1. Given

sufficient pressure drop across the nozzle, supersonic flow speeds become possible in the divergent region. Once they do, the one-dimensional relationships indicate that the convergent section of the nozzle accelerates subsonic flow while the divergent section accelerates supersonic flow. To maintain acceleration at all points along the nozzle, the flow in the region of minimum area must be at Mach 1 [34]. This is a completely one-dimensional explanation, but it is nevertheless instructive. One-dimensional flows are those where all the important flow properties (density, pressure, temperature, etc.) are related to their pre-expansion values through a single parameter, in this case the Mach number. Laval nozzle design is usually considered to consist of the region downstream of the throat, since the design of the convergent and throat areas is less critical to good performance. The initial part of this section of the nozzle increases in diameter very rapidly and much of the acceleration to the terminal supersonic Mach number is accomplished here. Next there is a region of source flow where the streamlines are linear and radiate out from an apparent source point. Finally, there is a region within the nozzle where the residual effects of the initial rapid expansion are removed from the flow, the Mach number is accelerated to its final value, and the streamlines are made parallel. The density, pressure and temperature are constant everywhere in the subsequent flow.

At present, we employ the axisymmetric supersonic flows emerging from Laval nozzles for the study of neutral–molecule reactions, having focused upon the reactions of the OH radical. This technique has been the focus of an extensive review, both regarding flow generation and characteristics as well as chemical application [5]. In our application, flows from two separate pulsed nozzles are mixed in a small stagnation region. The flows contain buffer gas, neutral reactant (1–5%) and radical precursor (0.1–1%). A low current discharge is struck in this region to generate the radicals. The mixed gas then flows through a constriction of 1 cm diameter, reaches a flow velocity equal to the local speed of sound (Mach 1) and accelerates into the expanding region of a Laval nozzle. As mentioned, the walls of the Laval nozzle are precisely shaped to accomplish a number of important flow characteristics. First the gas accelerates and adiabatically cools during the expansion. The walls of the nozzle are sloped such that this expansion occurs without turbulent detachment from the laminar boundary layer forming at the nozzle surface. The latter portion of the nozzle surface slows the rate of cooling and redirects the flow streamlines to parallelism. Of course, whenever a supersonic gas is influenced by a subsonic object (the nozzle wall in this case or, more precisely, the subsonic boundary layer which is being reshaped by the nozzle wall), a shock wave is set up. The nozzle is designed such that these developing shock waves destructively interfere and do not propagate beyond the boundary layer. Finally, the nozzle is designed to reach completely parallel flow in the supersonic core at the same time that the design Mach number (the ratio of the hydrodynamic flow velocity to the local speed of sound) is reached. At this point the nozzle is terminated and the flow is allowed to exit into a pressure-matched chamber.

This entire discussion is complicated by the fact that real gases exhibit viscous and heat-transfer effects. To treat this problem, one must consider the effects that the walls have upon the flow. The concept of a boundary layer is introduced in which the flow is somewhat arbitrarily divided into a section where the effects of the wall are considered and a section where they are not. In the design of the nozzle, a numerical calculation is conducted which gives a boundary layer displacement thickness, the effective distance normal to the wall at which the effects of the wall on the flow can be considered to have abated. The displacement thickness must be added to the isentropic

solution above to generate the physical nozzle wall contour. The nozzles must be designed so that they not only lead to stable parallel flow but also must accomplish this for real gases in the presence of a growing viscous boundary layer at the nozzle wall.

The supersonic gas flow punches a path into the subsonic gas forming a cylindrical shock sheath around it. This sheath serves to buffer the supersonic flow from the background and acts like a gaseous wall to the flow. With background and flow pressures carefully matched, the supersonic flow continues in a parallel axisymmetric fashion without changes in the local pressure, temperature or density. It is this post-nozzle flow region that we employ as a kinetic laboratory. The temperature and pressure are determined by the nozzle Mach number according to the adiabatic relationships in equations (1) and (2).

Because of the constraints imposed by the gas non-idealities, a given nozzle must be designed for one particular pressure–temperature pair for a given set of initial conditions. In other words, one can design a certain Mach number nozzle to give stable flow at a given stagnation temperature only for one stagnation pressure, thereby fixing the final temperature and pressure by the relationship to the Mach number. By varying the stagnation temperature there can be found new stagnation pressures which result in stable flow at the new condition. Thus, any one nozzle can map out a curve in pressure–temperature space. By varying the stagnation temperature, it is then possible to obtain a kinetic environment over a range of final temperatures. If one wishes to vary the final pressure over a fixed temperature (or the temperature over a fixed pressure), it is necessary to do this with a number of nozzles. Each newly designed nozzle can then map new curves in P–T space, and with only a few nozzles it is possible to create overlapping temperature windows ranging from near 300 K to below 50 K.

Using either mass spectrometry or laser spectroscopy detection schemes, it is possible to monitor specific molecular or atomic densities in the post-nozzle flow. Since the temperature and flow velocity are constant in this region, the concentration or density as a function of distance map directly into loss or gain rate coefficients under the local thermal conditions. Using stagnation region discharges, we have generated the OH radical in these flows and studied a wide range of OH relaxation and reaction processes in this manner. Some of this work will be the topic of section 4.

3. Ion–molecule collisions

3.1. *Ternary molecular association*

Growing interest in the temperature dependence and microscopic mechanism of molecular association reactions provided a strong driving force for the initial development of very-low-temperature kinetic techniques. The strong inverse temperature dependence of the rates for association processes and the predicted importance of radiative association reactions in the synthesis of key small molecular cations in the cold interstellar medium are two reasons why association reactions have been studied by nearly every laboratory investigating low-temperature chemistry. In addition, these reactions involve processes that would appear to be simpler in nature than electron or atom transfer reactions. Association studies require only the stabilization of a single bond and the reaction is typically believed to occur on a single potential energy surface. Association processes then form a natural class of systems in which one has the potential from their study to learn basic aspects regarding low-energy collision processes, with the hope that this knowledge can then form the bases for extension to the more complex bimolecular reaction systems.

Ternary molecular (termolecular) association rate coefficients in cationic systems such as

$$N_2^+ + 2N_2 \rightarrow N_4^+ + N_2 \tag{3}$$

and

$$O_2^+ + 2O_2 \rightarrow O_4^+ + O_2 \tag{4}$$

display a strong negative temperature dependence. This dependence has long been experimentally characterized using the fitting law

$$k_3 = CT^{-n}, \tag{5}$$

where C and n are largely found to be temperature independent. Excellent reviews exist on the temperature dependence of these reactions above 80 K [35–37]. In general, the constants C and n are found to scale qualitatively upwards with increasing molecular complexity of either of the reactants. The value of n for a variety of such reactions is found to vary from 0.4 to nearly 6. Precise experimental determination of n has proven to be somewhat problematic in several cases, owing mainly to a limited temperature range of determination. In order to understand better the importance of this parameter, it is useful to look at a more detailed picture of the association process.

It is generally accepted that, in the simplest description, ternary molecular ion association can be described by the following mechanism:

$$A^+ + B \underset{k_b}{\overset{k_f}{\rightleftharpoons}} (AB)^+, \tag{6a}$$

$$(AB)^+ + M \xrightarrow{\beta k_s} AB^+ + M. \tag{6b}$$

The first step in the process involves the bimolecular formation of a metastable collision complex $(AB)^+$ which lies above the AB^+ dissociation energy. This formation rate is characterized by a rate coefficient k_f. That this complex lives in most instances many times greater than the vibrational period along the A–B coordinate is a manifestation of the internal structure inherent in A and B. If A or B has internal manifolds in which energy may be stored, energy flow into these degrees of freedom during the collision process removes energy from the dissociative coordinate. Thus the complex is temporarily bound with respect to dissociation until sufficient energy can recouple to this degree of freedom from the bath modes in A and B.

Since the entrance valley toward formation of a loose AB^+ collision pair is dominated by the attractive long-range ion–neutral molecule potential, it is not expected to possess any chemical barriers lying at a positive energy. The dissociation limit of AB^+ then converges onto zero-kinetic-energy reactants A^+ and B or, in the $(AB)^+$ formation process, all the incoming kinetic and internal energy of A^+ and B add to this dissociation energy of the complex. In the most general treatment, this energy is considered to be completely available for back dissociation to reactants through energy randomization within the transient complex. Depending upon the angular momentum content of the complex and the accessible rotational states of the dissociated reactants, the only barrier that must be surmounted on dissociation is the centripetal barrier. Averaged over all collisions and possible exiting angular momentum states, the inverse of this dissociation rate coefficient k_b is then the mean lifetime of the complex $(AB)^+$.

If the complex survives long enough to undergo a collision with a third body, M, energy transfer from the excited complex to internal states of M and the relative

$M-AB^+$ translation is highly probable. If the quantity of energy transferred is in excess of the negative binding energy of the complex, the outcome of this stabilization collision will be the formation of an AB^+ molecular ion lying below the dissociation limit. This complex negative bonding energy is equal to the difference between the energy of the top of the centripetal barrier and the asymptotic total collision energy. The rate coefficient for this stabilization step (ignoring, here, the process of collisional fragmentation of newly stabilized AB^+ molecules) is given by βk_s. Here, βk_s can be considered to be a simple collision rate coefficient and β is a measure of the probability for successful energy transfer out of the transient ion–molecule collision pair. The quantity β is actually an average over all possible stabilization processes and all energetic $(AB)^+$ pairs. These channels include stabilization to both states lying below the true dissociation limit as well as some subset of stabilization steps which terminate above the limit but whose states are trapped by the centripetal barrier. Although it is useful in many arguments to consider β as a separate measurable entity, one must be careful to consider its potential pressure and temperature dependence and, in particular, the complex set of dynamics over which it is an average.

The newly born AB^+ will eventually internally cool further via subsequent relaxation collisions and radiative processes. In most molecular ion systems, the AB^+ dissociation energy is in excess of 0.5 eV and can be as much as 3 eV or more for covalently bound systems. At low temperatures, this dissociation energy is much greater than the mean collision energy or the mean internal energy of the incoming third body. Therefore the probability that, during a hard third-body collision, sufficient energy flows into internal and kinetic energy of the subsequently departing M sufficient to stabilize AB^+ should statistically be quite high. The value of β should then be near unity at low temperatures and should be temperature insensitive.

The steady-state approximation leads to a connection between the overall ternary association rate coefficient k_3 and these elementary rate coefficients:

$$k_3 = \frac{k_f \beta k_s}{k_b + \beta k_s M}. \tag{7}$$

Although detailed investigations into the high-temperature and high-pressure behaviour of the stabilization process exist, the simplest connection between experiment and theory at low temperatures can be made in the low-pressure unsaturated regime where this relationship reduces to

$$k_3 = \frac{k_f \beta k_s}{k_b}, \tag{8}$$

and $k_3(M) \ll k_f$. For non-polar neutral species B and M, the collision rate coefficients k_f and k_s are similarly expected to be temperature independent and the complete temperature dependence of k_3 for such systems would appear to be contained solely in k_b and describe the energy dependence of the unimolecular dissociation rate of the unstable $(AB)^+$ collision pair. Comparison of the state densities between $(AB)^+$ and free thermal $A^+ + B$ support the supposition of the statistical nature of the AB^+ internal energy distribution and most models have taken this approach towards the calculations of k_3 [38–40].

The modified thermal model developed independently by both Bates [39] and Herbst [40] represents such a statistical approach to k_b. The model uses the Rice–Ramsperger–Kassel–Marcus (RKKM) formalism developed by Troe [41] to

calculate the internal partition function of the energized complex. In this way, the equilibrium between dissociated reactants and complex can be determined and the dissociation rate calculated. The results are then cast into a form

$$k_3 = CT^{-(p+\delta)}, \tag{9}$$

where p is a measure of the relative state densities between collision pair and reactants and thus increases with increasing collision pair complexity. The parameter δ is included to account for any temperature dependence in the stabilization step and is expected to be small in the low-temperature limit. For diatomic ion diatom collision pairs, p is calculated to be 2.00 or 1.75 depending upon whether the complex is linear or nonlinear respectively.

Of course, in any ion–molecule collision at non-zero impact parameter, the pair will bring into the collision centripetal angular momentum, and this can lead to a significant barrier to complex formation. This orbital angular momentum, together with that brought in by the separate rotational energies of the reactants, contributes to a total system angular momentum which must be conserved throughout the entire collision and subsequent back dissociation.

For a given complex, only some subset of the total excess internal energy is then available for dissociation. The phase-space theory application of Chesnavich and Bowers [38] to these processes more generally accounts for this detailed nature of the available state density and conservation restrictions. They applied the phase-space model originally developed by Light [42] to calculate k_b as a function of both energy and angular momentum of the $(AB)^+$ complex. Proper averaging over all collisions leading to complex formation then allows determination of the thermal rate coefficient $k_3(T)$. The bulk of the low pressure results from application of this model to real systems also predicts a strict inverse temperature rate law as given in equation (4), and the values of n are found to be similar to those predicted from the modified thermal model.

There is then a strong theoretical basis for the characterization of termolecular association rates by a simple T^{-n} scaling law, and measures of n can provide some insight into the averaged properties of a molecular complex. In addition, within these models, one makes a physical connection with the averaged complex lifetime. These values allow predictions of rates for other processes that proceed through statistical complexes, in particular radiative association events [43–46].

One of the first very-low-temperature rate studies involved a determination of the low-pressure limiting behaviour of $k_3(T)$ for the reactions

$$N_2^+ + 2N_2 \rightarrow N_4^+ + N_2 \tag{10}$$

and

$$O_2^+ + 2O_2 \rightarrow O_4^+ + O_2 \tag{11}$$

Above 50 K, reaction (10) was found to be well fitted by a T^{-n} rate law; however, significant deviations were found for reaction (11) below 80 K [47, 48]. It was observed that, at the lowest temperatures, a lessening of the temperature dependence occurred with the appearance that k_3 may become temperature independent or even decrease with decreasing temperature below 60 K. This very surprising result led to a significant controversy as to the origin, with a very simple but compelling argument given by Ferguson [49] which provides evidence that termolecular rate coefficients cannot manifest low-temperature maxima. The essentially thermodynamic argument is based upon the idea that internally excited complexes are expected to dissociate preferentially

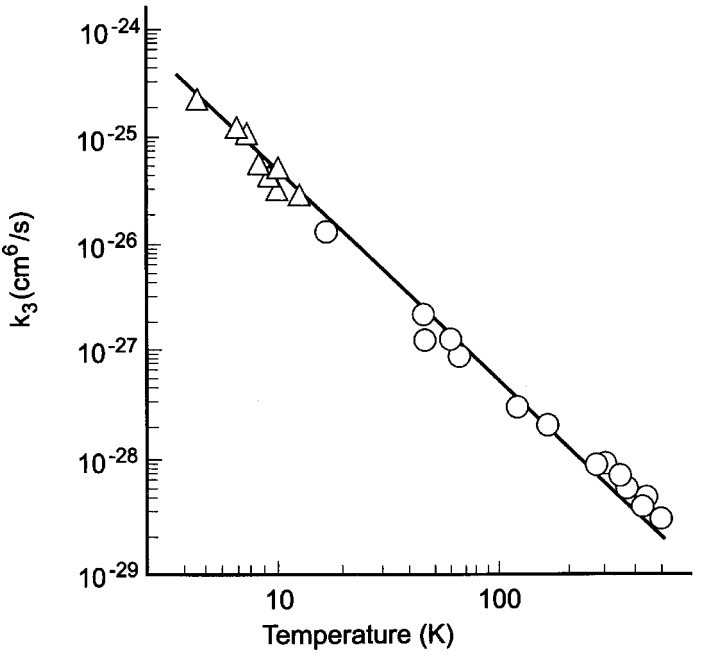

Figure 3. The temperature dependence of the termolecular rate coefficient for the association of N_2^+ with N_2 in an N_2 buffer. The data represent measurements in an axisymmetric supersonic flow reactor (CRESU) [4] (○) and a free jet expansion [51] (△).

to relatively cold products and therefore the activation energies for an ensemble of complexes is less than the strict dissociation energy of a ground-state AB^+ molecule. Using microscopic reversibility, Ferguson then shows that the bulk termolecular rate coefficient must continue to increase monotonically with dropping collision energy or temperature.

Rowe *et al.* [4] used the CRESU (cinetique de reaction en ecoulement supersonique uniforme, which means reaction kinetics in uniform supersonic flow) technique to study both reaction (10) and reaction (11) between 20 and 160 K. Again, for reaction (10) a good fit to an inverse temperature law down to 20 K was obtained. Experimental difficulties regarding O_4^+ break-up on sampling led only to the determination of lower bounds to the rate coefficient for reaction (11) below 70 K, the region where it had earlier been suggested a maxima existed. In spite of these difficulties, the CRESU data did not support any evidence for a maximum in $k_3(T)$ for this reaction. The free jet flow method has also been used to investigate reactions (10) and (11), as well as the association of a variety of other cations down to 1 K [50–54]. The results show excellent agreement with a strict T^{-n} rate law applying to all temperatures investigated. The combined low-temperature results for the absolute values of $k_3(T)$ for reaction (4) are shown in figure 3 with the results of a phase-space calculation for a nonlinear N_4^+ complex. It is very clear that the simple statistical models for molecular ion association apply quite well to this reaction at all temperatures investigated and that there must be a systematic problem with the lowest-temperature drift tube data on this system. In all other reactions, the low-temperature results reported to date fit an inverse temperature law quite well [3]. It would appear that our simple ideas regarding the statistical nature of molecular association at the lowest of temperatures remains consistent with observation.

Combined with the assumption of unit efficiency stabilization of the complex upon third-body collision, we can use the results to calculate the average lifetime of these collision pairs. At 10 K, the average lifetime for the O_4^+ complex is determined to be 10 ns, while for the six-atom $C_2H_4^+$ complex formed from the association reactions of $C_2H_2^+$ with H_2 the lifetime increases to in excess of 150 ns. These extremely long collision times and their strongly nature with lower temperature and increased molecular complexity add strong support for the importance of radiative processes in molecular ion collisions at very low temperatures. Employing ion traps, initially Barlow *et al.* [55, 56] and more recently Gerlich and Horning [46] have directly observed bimolecular ion formation at low temperatures and densities attributed to radiative association processes. Such processes have long been postulated to be important in the initial formation of small molecular species in highly rarefied interstellar gas clouds where gas-phase ternary processes are insignificant.

3.2. *Charge-transfer reactions*

Electron-transfer reactions have long held a special place in mechanistic chemistry. Their non-adiabatic nature does not permit us to use the simpler concept of chemistry as proceeding via trajectories on single Born–Oppenheimer potential surfaces. In this way our understanding of electron transfer reactions conflicts with much of our trained reasoning regarding atomic and molecular interaction. These reactions by nature must involve interaction of atomic and electronic motion or, in other words, the interaction coupled through nuclear motion of at least two independent Born–Oppenheimer surfaces. This unique feature has made their study a challenge towards the elucidation of the full nature of this electronic–nuclear motion interaction [57]. Extensive study of such systems has made them some of the most experimentally well characterized, if not still least understood, of all chemical reaction classes. The predominant problem is not of bulk mechanism as much as it is about microscopic action, the positions along trajectories where these crossings occur and the full descriptions of the motions that aid in the transitions. The predominance of charge-transfer processes in the set of ion–molecule reactions displaying dramatic temperature dependences has allowed low-temperature studies to contribute to this field.

Several charge-transfer systems display anomalously low rate coefficient values at elevated temperatures. Most notable are the reactions

$$N_2^+ + O_2 \rightarrow N_2 + O_2^+ \tag{12}$$

and

$$Ar^+ + O_2 \rightarrow Ar + O_2^+. \tag{13}$$

In reaction (12), a 300 K rate coefficient value of 5×10^{-11} cm^3 s^{-1} has been measured [58]. Gaucherel *et al.* [59] measured rate coefficient values for this reaction which displayed a continuous increase as temperature was lowered from 160 to 8 K. The rate coefficients were observed to reach a plateau of 3.5×10^{-10} cm^3 s^{-1} at the lowest temperatures. This plateau is supported by independent measurements of Randeniya and Smith [60] near 10 K. The combined results are shown in figure 4. The inverse temperature dependence is consistent with a weak coupling between the reactant and product potential surfaces which must lie within the configuration space accessed by the N_2^+–O_2 collision complex. Using this simple model, Randeniya and Smith could quantitatively account for the full temperature dependence of the reaction between 8 and 300 K. The results of the model are given by the broken curve.

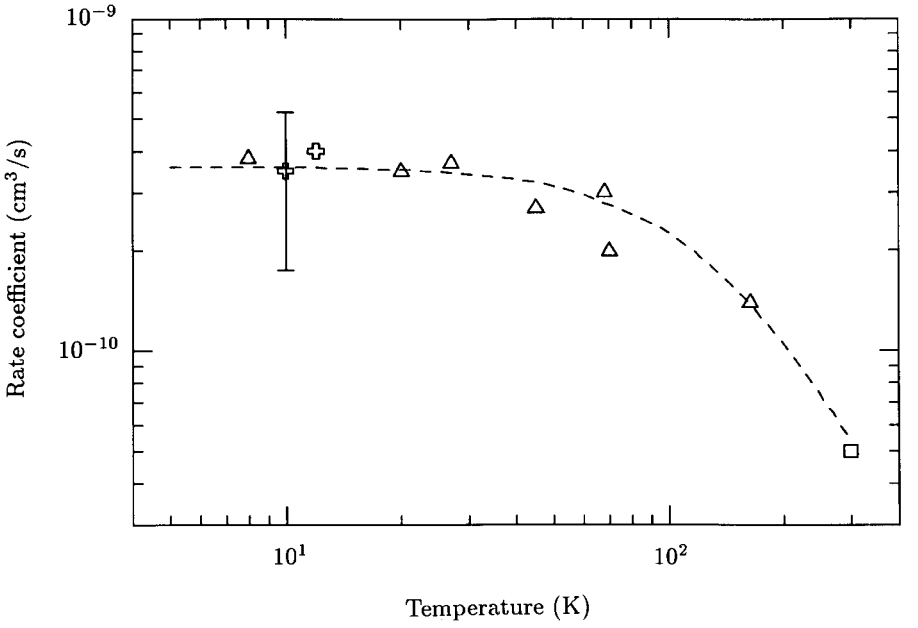

Figure 4. Rate coefficients for the charge transfer reaction of N_2^+ with O_2. The data result form measurements in a flowing afterglow [58] (□), the CRESU [59] (△) and a free jet [60] (✣). The broken curve represents a fit to a complex mediated model of Randeniya and Smith [60].

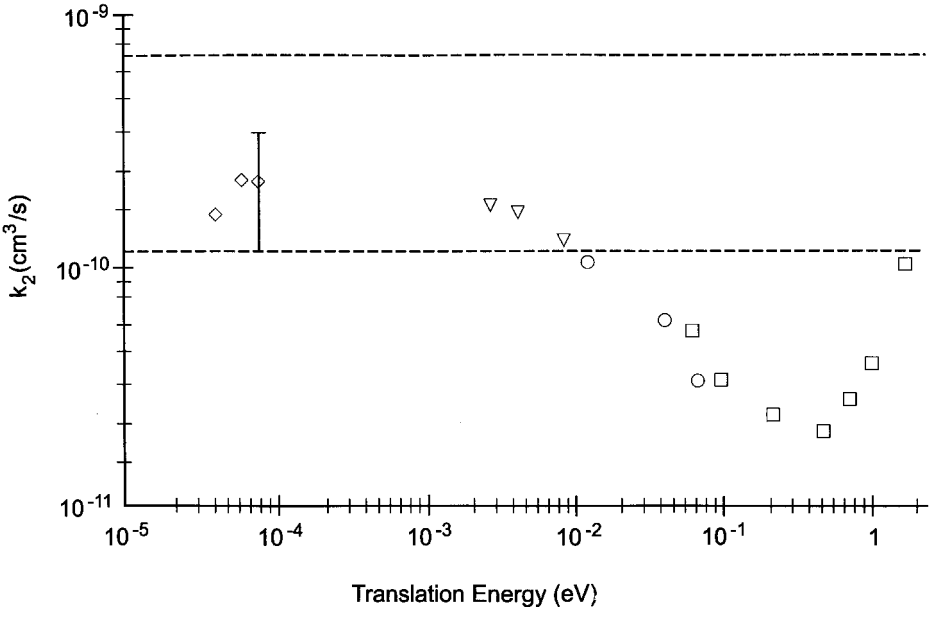

Figure 5. The translational energy dependence of the rate coefficient for the charge-transfer reaction of Ar^+ with O_2. The data were obtained from measurements using a guided ion beam scattering instrument [61] (□), a drift tube [58] (○), the CRESU [17] (▽) and the free jet [62] (◇).

Reaction (13) has been studied at very low temperatures using three independent techniques (see figure 5). Gerlich and Kalmbach [61] have reported the measurement of the rate coefficient for kinetic energies from 3 eV down to 1 meV as determined in a merged ion neutral beam apparatus. Their data show the well established minimum of 0.2 eV corresponding to the closing of the product channel yielding the O_2^+ $a^4\,\Pi$ state as the energy is lowered. As the energy is decreased further, the rate coefficient is seen to increase smoothly to an asymptotic plateau below 0.1 eV. This behaviour is entirely analogous to the low-energy behaviour of reaction (12), only shifted to higher energies or shorter-lived complexes. This certainly implies that there is no barrier for accessing the potential seam leading to products and most probably also implies that the potential coupling between the reactant and product surfaces is much stronger in this system. At very low energies, the data of Gerlich and Kalmbach indicate a rate coefficient value near 1×10^{-10} $cm^3\,s^{-1}$. Hawley and Smith [62], using the free jet flow method, and Rebrion *et al.* [17], using the CRESU method, have also investigated this reaction. The CRESU results obtained at 20, 30 and 70 K show a mild inverse temperature dependence with a rate coefficient value of 1.7×10^{-10} $cm^3\,s^{-1}$ at 20 K. The free jet data, all below 3 K, show a nearly constant rate coefficient of $(2.3\pm1.2)\times10^{-10}$ $cm^3\,s^{-1}$. Calculations have shown that, of the 12 degenerate potential surfaces corresponding to the complex, only two of them converge to a bound collision complex, that being the collinear ArO_2^+ state [63]. All others correlate to repulsive surfaces not expected to support a long-lived collision. Thus, in the absence of non-adiabatic coupling of these surfaces, only one sixth of all collisions should lead to a complex that can evolve to the $Ar+O_2^+$ products. The observed data are consistent with this model. The inverse temperature dependence at low energies suggests a mechanism whereby a complex must form to aid the crossing to products. The convergence of the rate coefficient at the lowest energies to a value in agreement with one sixth of the Langevin capture rate, or 1.2×10^{-10} $cm^3\,s^{-1}$, supports this mode. It has been suggested that the observation of rate coefficients in excess of the statistical limit at the lowest temperatures, using the CRESU and free jet methods, may be indicative of spin non-conservation in the very-longest-lived complexes. Such non-conservation is well documented in ion–molecule charge transfers at higher energies [64].

3.3. *Energy-transfer processes*

The development of the monitor ion technique, which allows selective chemical titration of internally excited ions, has provided a simple chemical means for the study of vibrational relaxation in molecular ions [65–75]. From the results of such studies, an important model proposing a dual mechanism for ion vibrational quenching has emerged and has been reviewed by Ferguson [70]. At high kinetic energies it has been found that quenching proceeds by a non-adiabatic Landau–Teller mechanism controlled by the repulsive forces of the interaction potential [76, 77]. This model predicts that the collisional relaxation probability will increase with increasing kinetic energy and is well documented for neutral–neutral quenching systems as well as for ion–neutral systems at high kinetic energies. At low collision energies, however, the long-range attractive forces which are unique to ion–neutral potential surfaces govern the quenching through production of long-lived collision complexes. Potential anisotropy is also found to play a key role in this complex formation [78]. Vibrational pre-dissociation of these complexes is found to lead to a renewed efficiency for quenching collisions at low collision energies. A qualitative criteria for the dominance of this second mechanism, uniquely observed for ionic systems to date is that the mean

collision energy lies below the well depth for the bound ion–reactant complex. Statistical theories suggest that the quenching efficiency will scale inversely with collision temperature according to the available internal degrees of freedom of the colliding partners. Since the majority of ion relaxation studies have been measured at moderately high kinetic energies in drift tubes, this turn-over behaviour to a complex mechanism has only been clearly demonstrated in a few cases, most notably for the systems

$$O_2^+(v=1)+Kr \rightarrow O_2^+(v=0)+Kr \tag{14}$$

and

$$NO^+(v=1)+CH_4 \rightarrow NO^+(v=0)+CH_4; \tag{15}$$

these reactions display minima in their quenching rate coefficients at 0.2 eV [71] and 0.5 eV [75] collision energies respectively, followed by inverse energy dependence below these energies. An obvious conclusion of this mechanism is that one would expect all collision partners to relax molecular ion vibrational states with unit efficiency in the limit of zero kinetic energy. As the statistical lifetime of the collision complex tends to infinity, vibrational pre-dissociation will dominantly compete against adiabatic back dissociation to the excited ion.

Using monitor ion methods in the free jet flow reactor, we have investigated such behaviour for the quenching reactions [79]

$$NO^+(v=1)+He \rightarrow NO^+(v=0)+He, \tag{16}$$

$$NO^+(v=1)+Ar \rightarrow NO^+(v=0)+Ar \tag{17}$$

and

$$NO^+(v=1)+N_2 \rightarrow NO^+(v=0)+N_2. \tag{18}$$

All three of these relaxing species have been shown to be highly inefficient at 300 K. The use of our free jet flow kinetic technique has allowed us to probe the temperature dependence of this quenching efficiency below 5 K and the results have confirmed the predictions of the complex mechanism. Indeed, it is only at these low temperatures that He has ever been observed to quench vibrationally a molecular ion and one finds the efficiency of reaction (3) approaches unity below 1 K translational energy.

Briefly, a free jet flow is produced of a coexpanded mixture, in this study containing a relaxant buffer, 1% of NO, to act as the $NO^+(v=1)$ ion precursor and 3–10% of a monitor gas to detect the $NO^+(v=1)$ population, competitively with buffer quenching. The $NO^+(v=1)$ ions are produced by laser ionization after parallel translational and rotational cooling is complete in the expansion. The ionization scheme is a (2+1) resonantly enhanced multiphoton ionization of NO through the $E\,^2\Sigma$ $(v=1)$ state. Photoelectron studies of this process have shown that 90% of the ion population is produced in the $NO^+X^1\Sigma^+(v=1)$ state, with only small amounts of impurities in higher vibrational levels [80]. Since the radiative lifetime of this state has been measured to be 90 ms [81], and the mean time between collisions in the jet is of order 1 μs, monitoring the $NO^+(v=1)$ population over a 100 μs flow time will be sensitive only to collisional loss processes.

We then study, over the subsequent jet flow, the competitive loss processes

$$NO^+(v=1)+B \rightarrow NO^+(v=0)+B \tag{19}$$

and

$$NO^+(v=1)+M \rightarrow NO+M^+ \tag{20}$$

where B is the buffer gas relaxant species and M is an appropriate monitor gas molecule whose adiabatic ionization potential is in excess of that of NO and yet less

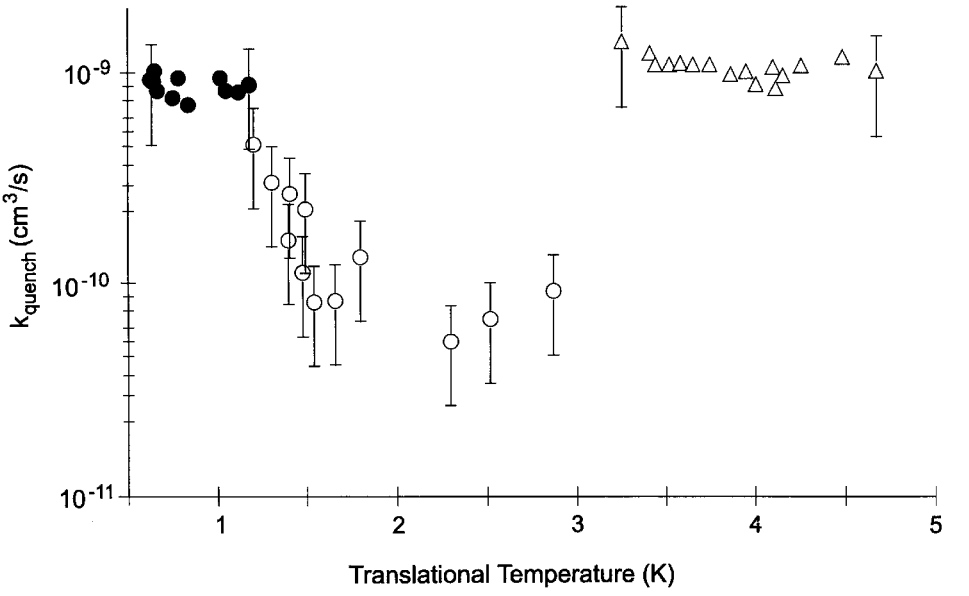

Figure 6. The temperature dependence of the NO^+ ($v = 1$) vibrational quenching rate coefficient for the relaxants N_2 (△), Ar (●) and He (○) measured in a free jet flow [79].

than the recombination energy of $NO^+(v = 1)$. Therefore, reaction (20) is only exothermic for vibrationally excited ions. We have assumed here that M does not act to relax $NO^+(v = 1)$ without electron transfer, and there are two monitor species that we have found which appear to meet this criterion.

The traditional monitor species for $NO^+(v = 1)$ has been CH_3I which has an ionization potential of 9.54 eV. The adiabatic ionization potential of NO is 9.25 eV, whereas the $NO^+(v = 1)$ recombination energy to produce vibrational ground-state NO is 9.55 eV, making reaction (20) 0.01 eV exothermic for CH_3I. This monitor has been used exclusively in the past for the higher-energy drift tube studies of $NO^+(v = 1)$ quenching. However, a recent ion cyclotron resonance study of the radiative lifetime of $NO^+(v = 1)$ using this monitor has suggested that the monitor reaction (20) in this case proceeds with less than 1% efficiency [81]. Our observations support this claim, at least in our very-low-kinetic-energy regime, and we find no evidence for the reaction of CH_3I with $NO^+(v = 1)$ below 5 K. It was therefore necessary for us to develop the use of alternative monitor species. The two that we settled upon for this study were C_2Cl_4 and C_2H_5I whose ionization potentials are 9.32 eV and 9.33 eV respectively. Although we cannot directly measure the rate coefficients for the corresponding monitor reactions at low temperatures (since we cannot perform the experiment in the absence of a buffer gas with its competing relaxation), all our observations of the mole fraction dependence of the monitor species on reactions (19) and (20) branching and the net rate of loss of $NO^+(v = 1)$ in the presence of monitor gas strongly suggest that these monitor neutrals charge transfer with $NO^+(v = 1)$ at the collision limiting value.

In order to determine the quenching rate coefficient for the buffer species we need only measure the terminal branching ratio of M^+ to NO^+ (all v) as a function of total stagnation pressure, monitor species partial mole fraction and the reaction distance between ion preparation and mass spectrometric detection. Self-consistent numerical solution of the integrated rate law under free jet conditions then provides the quenching rate coefficient k_q.

The results of our measurements are shown in figure 6. Clearly, the most striking feature of the present results is the high efficiency of vibrational quenching in the low-temperature limit. Quenching by both Ar and N_2 is found to have no temperature dependence and to proceed at a value near the collision limited value. Both of these relaxants display 300 K relaxation rates greater than 50 times slower than the Langevin value [79]. This strongly suggests that the Ferguson mechanism of quenching through complex formation is active in this regime. At low temperatures, each Langevin capture collision is producing a complex of sufficiently long duration such that vibrational predissociation can proceed with unit efficiency. It has been pointed out by Tosi *et al.* [82, 83] in a series of trajectory studies on ion–neutral vibrational relaxation that both well depth and potential anisotropy are important in driving these processes. In a statistical sense, the well depth, by governing the number of available complex states, will certainly control the collision complex lifetime at a given collision energy. The anisotropy, in addition to adding to the complex formation rate, apparently also aids the conversion of vibrational energy into product rotational states and in a classical sense can help to drive the pre-dissociation.

Another startling result of this study regards the fact that He appears to lead to nearly unit quenching efficiency at these low collision energies. The observation of a measurable He quenching rate has never been made at higher temperatures owing to its weak interaction as a result of very low polarizability. This low polarizability will effect a weak complex binding energy but will also greatly reduce the anisotropy of the potential. Coupled with the disparate mass combination between NO^+ and He, in a purely classical sense He would be expected to be a very poor agent for transforming NO^+ vibrational energy into NO^+ rotational energy. These arguments certainly support the low ambient efficiency of He as a relaxant. However, at 1 K it clearly appears that the duration of the complex is sufficient for even these weak pre-dissociative forces to begin to dominate. From the apparent temperature dependence of the quenching efficiency at these low temperatures, it is also clear that relaxation by He will only be important at the very low thermal conditions of free jets and in other sub-10 K environments.

Adams *et al.* [84] have studied the reactions of Kr^+ and Xe^+ in both fine-structure states ($^2P_{1/2}$) and ($^2P_{3/2}$) with several gases at 300 K using a selected-ion flow tube apparatus. They observed fine-structure relaxation of $Xe^+(^2P_{1/2})$ in collisions with CH_4 and N_2O, but not with O_2, OCS, H_2S or NH_3. Disappearance of Xe^+ proceeds at 90% of the collision rate for both CH_4 and N_2O collision partners with branching ratios of 50 : 50 and 75 : 25 for the charge transfer to electronic quenching collisions of $Xe^+(^2P_{1/2})$. No $Kr^+(^2P_{1/2})$ electronic quenching was observed for any of the collision partners in the study. $Kr^+(^2P_{1/2})$ relaxation by N_2 has been studied by Lindinger [85]. Although the quenching collision is exothermic, the quenching rate coefficient is shown to increase monotonically from 6×10^{-12} cm^3 s^{-1} to 2.7×10^{-11} cm^3 s^{-1} in the centre-of-mass collision energy regime of 0.06–0.44 eV. The positive temperature dependence is anomalous and absence of a minimum in k_q against KE_{cm} suggests the interaction between $Kr^+(^2P_{1/2})$ and N_2 is primarily repulsive, or any attractive well must be less than approximately 100 meV deep.

We have explored the very-low-collision-energy regime of $Xe^+(^2P_{1/2})$ relaxation in the core of a free jet expansion apparatus employing time-of-flight mass spectrometry detection [86]. Since our time-of-flight detection system cannot directly measure the fine-structure distribution of Xe^+, a chemical monitor method was employed to differentiate between the fine-structure states by competitive charge-transfer chem-

istry. CH_4 and/or N_2O were used to monitor the concentration of $Xe^+(^2P_{1/2})$ by charge transfer as their ionization potential lies between the ionization energies required for Xe^+ $(^2P_{1/2})$ and $Xe^+(^2P_{3/2})$ production from Xe. We find that non-reactive collision partners produce little fine-structure quenching whereas collision partners with exoergic charge transfer channels react with $Xe^+(^2P_{1/2})$ on every collision and via a double-charge-transfer mechanism efficiently produce $Xe^+(^2P_{3/2})$ below 10 K collision energies.

The ionization potentials of both CH_4 and N_2O lie between $Xe^+(^2P_{1/2})$ and $Xe^+(^2P_{3/2})$, and in both cases substantial amounts of molecular product ions are observed during the quenching studies with these partners. In addition, quenching rate coefficients are measured to be significant at 61% and 16% of the collision rate for CH_4 and N_2O, respectively. Quenching appears to be facilitated by the open charge-transfer channel. All other quenching agents investigated had ionization potentials lying below that of Xe and showed no detectable quenching efficiency. It appears that a charge-transfer reaction greatly facilitates fine-structure relaxing collisions in $Xe^+(^2P_{1/2})$. Even at extremely low collision energies, neither increased polarizability nor increased collision complex degrees of freedom seems to facilitate quenching in contrast with observed increased non-adiabatic efficiencies for many other reactions at low temperatures [3]. These other reactions include both ion–molecule charge transfer and molecular ion vibrational relaxation. Both CH_4 and N_2O, exhibiting electronic quenching, have total reaction rate coefficients for loss of $Xe^+(^2P_{1/2})$ equal to the Langevin collision rate coefficient. The absence of a significant temperature dependence in the quenching rate coefficient supports a mechanism whereby electronic quenching in these systems is proceeding via a sequential double-electron-transfer mechanism.

3.4. *Enthalpically driven chemistry*

While investigating the fine-structure relaxation of $Xe^+(^2P_{1/2})$ by SF_6 using CH_4 as a monitor we observed formation of a significant amount of HSF_6^+ as a terminal proton-transfer product ion [87]. With the exception of one observation of HSF_6^+ comprising approximately 0.1% of the total ion signal in a flowing afterglow apparatus [88], HSF_6^+ has not been considered an isolable ion. The proton affinity always has been inferred from thermodynamic data involving the appearance of SF_5^+ as a dissociative proton transfer product. Our observation of stable HSF_6^+ near 0 K prompted a bracketing study using competitive proton-transfer chemistry to determine the proton affinity of SF_6.

The very-low-temperature proton-transfer chemistry was performed within the core of a free jet. The primary proton source ion, H_2^+ $(v = 0)$, was produced by 3+1 REMPI through the $\tilde{C}$ $(v = 0)$ state [89]. The remaining proton donor ions, shown in table 1, were prepared by proton transfer from H_2^+. Seeding SF_6 into these expansions at low concentrations allows kinetic separation of the desired proton-transfer reactions

$$H_2^+ + R \rightarrow RH^+ + H, \tag{21}$$

and

$$RH^+ + SF_6 \rightarrow R + HSF_6^+ \tag{22a}$$

$$\rightarrow R + HF + SF_5^+. \tag{22b}$$

Time-of-flight mass spectra as a function of reaction time were collected and analysed to determine the branching ratio k_{22a}/k_{22b}.

The branching ratio between reactions (22*a*) and (22*b*) with donor molecules of varying proton affinities are shown in table 1. The fact that HCO^+ leads to no reaction

Table 1. Proton affinities at 298 K for several proton donors and products of the reaction of the protonated donor with SF_6 [87].

Reactant HM^+	Proton affinity of M (kcal mol^{-1})	Products
HCO^+	141.4	No reaction
HN_2O^+	137.3	HSF_6^+
HCH_4^+	130	HSF_6^+
HCO_2^+	128.5	HSF_6^+
HCF_4^+	126.5	HSF_6^+
HN_2^+	118.2	HSF_6^+(13± 3%)
		SF_5^+(87± 3%)
H_3^+	101.3	HSF_6^+(2± 2%)
		SF_5^+(98± 2%)
HAr^+	88.6	SF_5^+
H_2^+	61.1	SF_5^+

with SF_6 and reaction of HN_2O^+ with SF_6 yields solely HSF_6^+ strongly suggests that the proton affinity of SF_6 lies between that for N_2O and CO. One does not expect these simple proton-transfer reactions to possess positive activation barriers and all exothermic proton transfers are expected to proceed at the collision limit at low temperatures. With regard to bracketing the proton affinity of SF_6, the measurement in this experiment determines the sign of the free energy change for reactions (22*a*) and (22*b*) at 5 K. Account of the small temperature dependence of the heat capacities for the species involved in the direct proton-transfer reaction leads to a 5 K proton affinity 137.9± 2.0 kcal mol^{-1} for SF_6. Within this accuracy there is no change in this value when further corrected to 0 K. Consideration of the heat capacities of SF_6 and HSF_6^+ then allows determination of the 298 K proton affinity as 139.3± 2.0 kcal mol^{-1} in agreement with the previous 298 K value of 138± 3 kcal mol^{-1}. As the proton affinity of the donors decreases, the exothermicity for the proton transfer to SF_6 increases and one begins to observe the dissociative channel, reaction (22*b*). From the threshold of HSF_6^+ fragmentation at a proton-transfer exothermicity of 21.2 kcal mol^{-1}, upper bounds to the heat of formation for SF_5^+ of 11.6 kcal mol^{-1} at 298 K, or 9.2 kcal mol^{-1} at 0 K, are obtained. This observation is consistent with the recently reported values of 2.7+ 5.4 kcal mol^{-1} (298 K) and 0.7± 5.4 kcal mol^{-1} (0 K) of Becker *et al.* [90] since our measurement represents an upper bound and may also reflect an activation barrier in the dissociation of HSF_6^+. The appearance energy of SF_5^+ at 298 K is determined to be 321.9 kcal mol^{-1} in agreement with the results of Tichy *et al.* [91].

The stability of HSF_6^+ at low temperatures with respect to dissociation to HF and SF_5^+ reflects an activation enthalpy of at least 12 kcal mol^{-1}, in agreement with the value of 10± 2 kcal mol^{-1} obtained by Mackay *et al.* [88]. Owing to the large positive entropy change for reaction (22*b*) of 37–43 cal K^{-1} mol^{-1}, depending on M, it is entirely the low-temperature nature of the current study that has allowed unambiguous HSF_6^+ observation. Chemistry near 0 K, under entropy-free conditions is governed solely by enthalpic forces. Under these conditions, reaction (22*b*) is endoergic. At 298 K the free energy of reaction for dissociative proton transfer (reaction (22*b*)) becomes dominated by the entropic term and drops to negative; the large open phase space for the dissociative pathway leads almost exclusively to SF_5^+ product ion from any proton-transfer processes to SF_6. Similar effects are observed in our laboratory for proton transfer to CF_4 to produce HCF_4^+ from HN_2^+. The HCF_4^+ ion has long been

known to be stable but to have a nearly isoergic path yielding $CF_3^+ + HF$ [92]. At 5 K we observe proton transfer from H_2^+ to yield primarily CF_3^+ (greater than 90%) but with the less energetic reaction

$$N_2H^+ + CF_4 \rightarrow N_2 + HCF_4^+; \tag{23}$$

the exothermicity of 8.3 kcal mol^{-1} appears to be insufficient to drive the fragmentation process. Although only providing lower bounds to such endothermic barriers, ion chemistry at very low temperatures can provide valuable insight into the true reaction mechanism and the driving forces behind this chemistry.

4. Molecular collisions

4.1. *Molecular association*

The temperature dependence of free-radical recombination reactions plays a critical role in the chemical dynamics and composition of planetary atmospheres, including our own [93–95]. These reactions often manifest strong inverse temperature dependences, with the reaction rate coefficients increasing with decreasing temperature, or even more complex dependences. Currently there is strong interest in the chemistry of hydroxyl-containing reservoir species such as nitrous and nitric acid. Nitric acid is specifically thought to be a chain-terminating product in at least one of the ozone depletion reaction cycles owing to its stability to oxidation. Furthermore, as a stable form of odd oxygen, it can act as a transport agent for OH in the stratosphere. The impact of strong seasonal variation in the stratospheric temperature over certain parts of the globe demands careful laboratory determination of the rates for reservoir species production reactions across a broadened range of temperatures.

Certainly two of the most atmospherically relevant association reactions of hydroxyl are those with nitric oxide and nitrogen dioxide:

$$OH + NO + N_2 \rightarrow HONO + N_2, \tag{24}$$

$$OH + NO_2 + N_2 \rightarrow HONO_2 + N_2. \tag{25}$$

These reactions are also important in combustion processes and have been extensively studied in the elevated- to near-ambient-temperature range (550–340 K) [96–99]. The negative temperature dependence in this window has been well explained using RRKM models [100]. These attribute enhanced low-temperature reactivity to the increased lifetime of the initially formed HONO collision complex at low collision energies. As a result, most of the laboratory findings have been fitted to a statistical model employing a $k = CT^{-n}$ dependence. Clearly an extension of the temperature range to much lower temperatures provides a sensitive and valuable test of these models. Additionally, the temperature extant in the upper atmosphere is only approached by the currently available data, and it is necessary to extend the temperature range of laboratory kinetic data well below 230 K.

For the hydroxyl radical reactions in a Laval post-nozzle flow, a cold-cathode discharge in a water vapour seeded flow was found to be useful OH production method [32]. At the nozzle exit, the OH was found by LIF, to reside solely in the lowest-energy states OH $X\,^2\Pi_{1/2,3/2}(v = 0)$. Clearly, collisions with water vapour and the buffer during the expansion process effectively cool the nascent OH. Rotationally resolved excitation spectra of the R_1 and R_{21} branches of the (0,0) band of the transition displayed rotational distributions well fitted to temperatures consistent with those predicted by the isentropic relationship for both nozzles. This demonstrates that the flows exhibit thermal equilibrium between all degrees of freedom owing to the

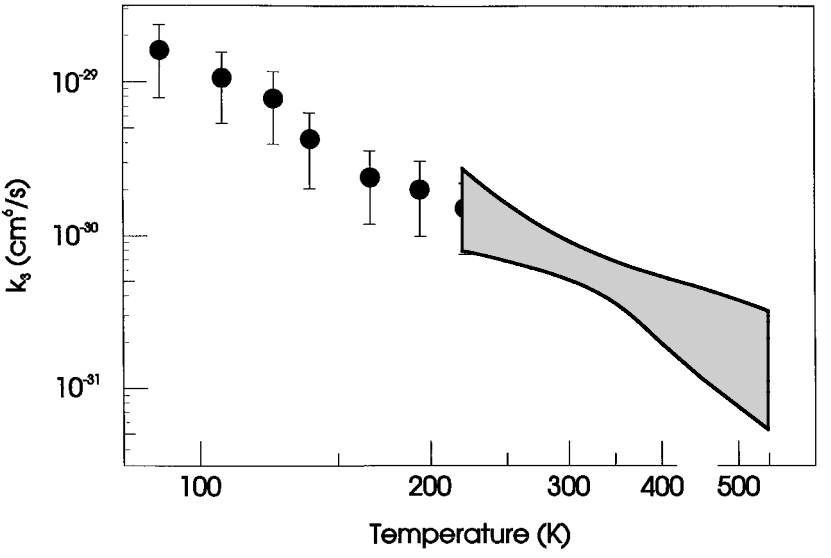

Figure 7. The temperature dependence of the low-pressure termolecular association rate coefficient for the reaction of OH with NO in a nitrogen buffer: (▨), recommendation of DeMore *et al.* [98]; (●), data obtained in the Laval flow reactor using various nozzles [32].

continuum nature of the flow. The OH density, monitored by observing the $R_1(2)$ line near 307 nm, was also found to be constant within 5% in the absence of added reactant, again demonstrating the uniform nature of the flow (at least on the centre streamline). As small fractions of NO are seeded into the flow, the OH LIF signal was observed to decrease with increasing distance in a pseudo-first-order manner. The observed rate was found to increase linearly with increasing NO concentration, allowing extraction of the absolute rate coefficient at a given total flow pressure. By maintaining relative NO fractions below 10%, the third body was N in the 10^{16}–10^{18} molecule cm^{-3} density range. Under these conditions, the reaction is near the low pressure limit, and the low-pressure absolute reaction rate coefficients are displayed in figure 7.

The shaded region in figure 7 represents the recommended temperature dependence of the rate coefficient including error from DeMore *et al.* [98]. The good agreement between our low-temperature measurements and the recommendation addresses several issues. First it would appear that the new technique reported here provides reliable rate coefficient information in the low-temperature regime which is not easily accessible via conventional kinetic methods. Second, it is evident that simple statistical interpretations of the reaction mechanism remain valid at low temperatures as manifested by the inverse power dependence of k_3 on temperature. Combining the new results with the high-temperature recommendation allows us to report a global temperature dependence for the termolecular association reaction. The new recommendation is $k_3 = 7.0 \pm 2.0 \times 10^{-31} (T/300)^{-2.6 \pm 0.3}$ cm^6 s^{-1} between 90 and 550 K.

4.2. *Atom-transfer reactions*

The reactions of atomic bromine and bromine oxide (BrO) are known to play key roles in the catalytic destruction of ozone in the terrestrial atmosphere [98]. The effectiveness with which a given radical destroys ozone through catalytic cycles, the

rates of conversion to stable sink or reservoir species and the regeneration of the active species determine its impact on stratospheric chemistry. The regeneration reaction

$$OH + HBr \rightarrow H_2O + Br \tag{26}$$

proceeds at a rate which is over an order of magnitude greater than the corresponding hydrogen chloride reaction at room temperature. This, in combination with many other factors, has the effect of increasing the ozone depletion potential of bromine beyond that of chlorine [101].

The first determination of the temperature dependence of the rate coefficient for reaction (26) was reported by Ravishankara *et al.* [102] in 1979. The rate coefficient was found to be independent of temperature in the 249–416 K range. Six different temperature points in this range were averaged to provide a recommended bimolecular rate coefficient $k = (1.19 \pm 0.14) \times 10^{-11}$ cm^3 s^{-1} applicable to this temperature window. Since then several groups, including that of Ravishankara, have remeasured the rate coefficient at 298 K and found general agreement with the recommended value at this temperature [103–105]. Recently, Sims *et al.* [12] measured the temperature dependence of the rate coefficient into the ultralow-temperature range (23–295 K) and found a strong negative temperature dependence. These data were fitted to a simple model derived from quantum scattering calculations [106], with the fit exceeding the accepted 250–300 K value by a factor of almost two. Additionally, the ultralow-temperature behaviour of this reaction has been predicted using statistical adiabatic capture theory [107].

The model derived from quantum scattering calculations gives the first theoretical attempt to describe the temperature dependence of the rate coefficient. These calculations were based on the rotating-bond approximation [108]. Clary considered the reaction

$$OH(j,k) + HBr(v) \rightarrow H_2O(m,n) + Br, \tag{27}$$

where j is the rotational state of OH, v is the vibrational state of HBr, while m and n are the bending mode and a local stretching mode quantum numbers respectively of the product H_2O. The potential energy surface used in this calculation was based on an accurate H_2O potential and on the transition state for the OH + HCl reaction found from a quasiclassical trajectory calculation. The rate constant was calculated from Maxwell–Boltzmann averaging over the cross-sections and the product with the initial velocity and then over all j values. This gives the following rate coefficient:

$$\begin{aligned} k(T) &= \left\{k_0(T)\left[1 + 2\sum_j \exp\left(-\frac{E_j}{k_b T}\right)\right]\right\} \Big/ \left[\sum_j (2j+1)\exp\left(-\frac{E_j}{k_B T}\right)\right] \\ &= k_0(T)\left(\frac{B\pi}{k_B T}\right)^{1/2} \end{aligned} \tag{28}$$

where $k_0(T)$ is the rate coefficient for OH($j = 0$), B is the rotational constant of OH and k_B is the Boltzmann constant. Given that the lower stratospheric temperatures relevant for OH and halocarbon chemistry extend to nearly 180 K and are routinely around 200 K, while the recommended rate behaviour is based predominantly upon data obtained above 240 K, careful re-examination of the rate coefficient at low temperatures is clearly necessary.

Both our group [13], as well as Sims *et al.* [12], have examined this reaction in a Laval flow. All the temperature-dependent rate data are shown in figure 8. The negative temperature dependence of the reaction below 200 K is clear, but the onset of

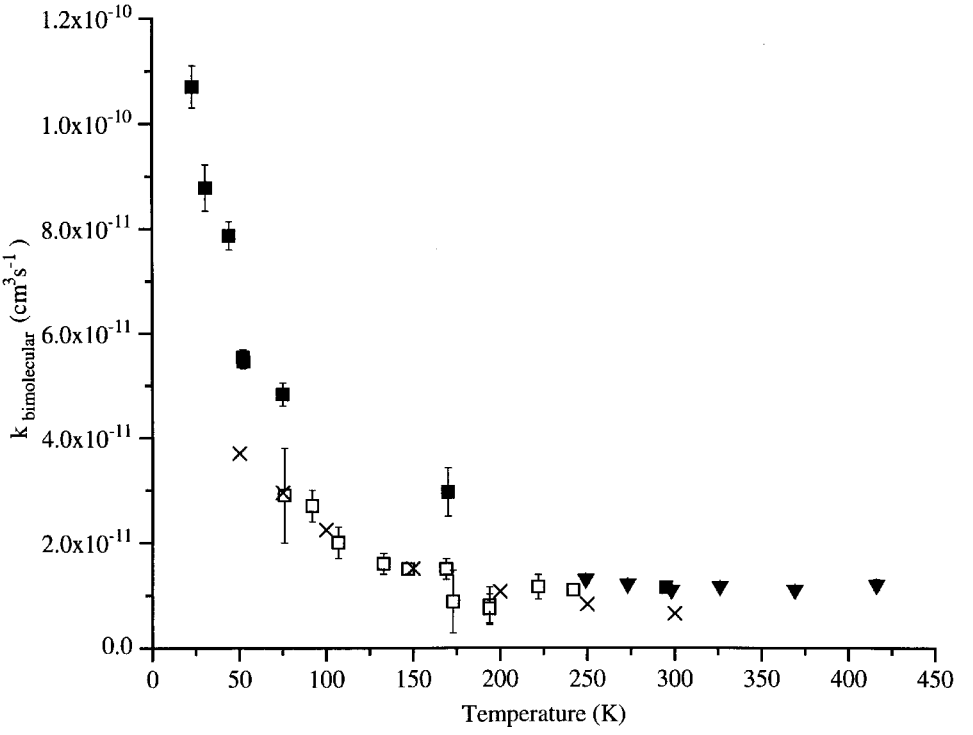

Figure 8. Temperature dependence of the bimolecular rate coefficient for the reaction OH + HBr: (▼), measurements in a conventional flow tube [103]; (■), measurements from an axisymmetric supersonic flow reactor [12]; (□), our work using a Laval nozzle flow [13]; (×), results of a quantum scattering calculation. [106].

this dependence is more gradual than reported earlier. Owing to the very recent and novel developments in low-temperature kinetic methodology, we cannot yet comment on the differences in results obtained in this work relative to those reported by Sims *et al.* who also employed an axisymmetric supersonic flow. The invariance of the rate coefficient over greater than an order-of-magnitude change in total pressure in our studies indicates that this reaction manifests entirely bimolecular behaviour at these temperatures, which is in line with the observations of Sims *et al.* The model for the temperature dependence of the rate coefficient (equation (28)) proposed by Clary, provides a good fit of the combined data of Ravishankara and this report, while observing only a small deviation from the data of Sims *et al.* The dominant $T^{-1/2}$ dependence of the model is a consequence of both the strong long-range dipole–dipole interaction potential and a $(2J+1)^{-1}$ dependence in the reactive cross-section, which causes OH rotational excitation to inhibit the reaction.

It may very well be that there exists a much better fitting law to explain the full range of the temperature dependence of the rate coefficient. This is seen at lower temperatures where statistical adiabatic capture theory seems to provide an upper limit to the exact rate constant since it assumes only a dipole–dipole interaction potential as well as accounting for the open-shell nature of the OH radical. However, one should not overemphasize the relationship between fitting laws and reaction mechanisms. The results of Clary *et al.* are providing the first insight into the importance of both dipolar interactions and rotational energy dependence of this

reaction system. It remains unclear as to the importance of competition between direct and collision complex mediated reaction in this system, as well as the subtleties of the energy dependences of both complex formation and complex dynamics.

The results indicate that there is clearly a strong reaction mechanism switching which is observed at temperatures below 150 K. One possibility for this switching would be the onset of molecular association to form the HOHBr complex. Sims *et al.* reported that at 52 K a twofold change in buffer density gave no rate change, consistent with a bimolecular reaction. At the higher temperatures of our study, changes in total density of greater than an order of magnitude also indicate bimolecular behaviour, although the contribution of termolecular processes would be expected to be much greater in the temperature window of the Sims *et al.* study.

At a fundamental level, it is interesting that the dynamics of such a simple reaction should show such a rich temperature dependence. Some mechanism change appears to be occurring at low temperatures, but its nature is as yet unclear. Elucidation of the mechanism active at low temperatures would certainly be aided by product detection, and efforts are under way in our laboratory to accomplish such characterization. The reaction also remains a useful challenge to high-level dynamic theory because of the interesting rate complexity, as well as the relative simplicity regarding the number of atoms. As such, the reaction will most probably continue for a while as a benchmark for temperature-dependent elementary radical–molecule reactions.

5. Conclusions and future directions

The field of low-temperature gas-phase chemistry, and in particular chemical rate studies utilizing the advantages of supersonic flows and expansions, is one now gaining an established record. Our understanding of the physical characteristics of these flow environments has grown rapidly, together with our ability to exploit those properties for unique collision studies. The various techniques have now been largely cross compared and their advantages and disadvantages made clear. The bulk of the kinetic development has been accomplished, and groups in this area are currently investigating the full breadth of chemistry which may be unveiled in this low-temperature window between 1 and 200 K.

There are several directions in chemical study that we shall see investigated in this area during the near future. We shall continue to see investigation of rate coefficients for direct application in the modelling of nature environments, particular planetary atmospheres and the interstellar medium. In this regard, we should see extension of the types of reactants being studied to those of high prevalence in these environments, such as the first-row atoms and their simple hydrides and oxides. Extensions will also be made towards the simple metal atoms and clusters to investigate the reactivity of dust-like aggregates at low temperatures.

We shall continue to see applications of these low-temperature environments for the extension of our understanding of inelastic collision processes in both ionic and neutral systems. These studies will be headed in the direction of very specific state-to-state cross-section measurements as a function of collision energy and state label. The goal is to pull together our observations of low-temperature rate enhancement into a detailed picture of the microscopic dynamics of atomic and molecular collisions in the 0 K limit.

Finally, we shall certainly begin to see new applications of low-collision-energy studies for the elucidation of various physical behaviours. In particular, studies are in progress to exploit the properties of long-lived collisions to allow new types of

spectroscopy for transient ions and radicals in the infrared and electronic regions of the spectrum. As new investigators enter this low-energy collision field, there will undoubtedly emerge other novel and illuminating developments in both techniques as well as molecular physics and chemistry.

Acknowledgements

The work in the author's laboratory directed towards these studies over the past decade has been funded by grants from the National Science Foundation as well as the Petroleum Research Fund administered by the American Chemical Society.

References

[1] Levine, R. D., and Bernstein, R. B., 1987, *Molecular Reaction Dynamics and Chemical Reactivity* (Oxford University Press).
[2] Baer, M., and Ng, C. Y., 1992, *State Selected and State to State Ion Molecule Reaction Dynamics* (New York: Wiley).
[3] Smith, M. A., 1994, *Advances in Ion Chemistry and Physics*, Vol. 1, edited by T. Baer and C. Y. Ng (New York: Wiley), p. 183.
[4] Rowe, B. R., Dupeyrat, G., Marquette, J. B., and Gaucherel, P., 1984, *J. chem. Phys.*, **80**, 4915.
[5] Atkinson, D. B., and Smith, M. A., 1995, *Rev. scient. Instrum.* **66**, 4434.
[6] Winnewisser, G., and Herbst, E., 1987, *Top. curr. Chem.*, **139**, 119.
[7] Black, J. H., and Dalgarno, A., 1973, *Astrophys. Lett.*, **10**, 17.
[8] Mitchell, G., Ginsberg, J. L., and Kuntz, P. J., 1978, *Astrophys. J., Suppl.* **38**, 39.
[9] Prasad, S. S., and Huntress, W. T., 1980, *Astrophys. J., Suppl.*, **43**, 1.
[10] Anicich, V. G., and Huntress, W. T., 1986, *Astrophys. J., Suppl.*, **62**, 553.
[11] Sims, I. R., Queffelec, J. L., Defrance, A., Rebrion Rowe, C., Travers, D., Bocherol, P., Rowe, B. R., and Smith, I. W. M., 1994, *J. chem. Phys.*, **100**, 4299.
[12] Sims, I. R., Smith, I. W. M., Clary, D. C., Bocherel, P., and Rowe, B. R., 1994, *J. chem. Phys.*, **101**, 1748.
[13] Atkinson, D. B., Jaramillo, V. I., and Smith, M. A., 1987, *J. chem. Phys.*, **101**, 3356.
[14] Clary, D. C., Haider, N., Husain, D., and Kabir, M., 1994, *Astrophys. J.*, **422**, 416.
[15] Herbst, E., and Leung, C. M., 1989, *Astrophys. J., Suppl.* **69**, 271.
[16] Gerlich, D., 1992, *State Selected and State to State Ion Molecule Reaction Dynamics*, Part 1, edited by C. Y. Ng and M. Baer (New York: Wiley), 1–176.
[17] Rebrion, C., Marquette, J. B., and Rowe, B. R., 1989, *J. chem. Phys.*, **91**, 6142.
[18] Hawley, M., Mazely, T. L., Randeniya, L. K., Smith, R. S., Zeng, X. K., and Smith, M. A., 1990, *Int. J. Mass. Spectrom. Ion Processes*, **97**, 55.
[19] Smith, M. A., and Hawley, M., 1992, *Advances in Gas Phase Ion Chemistry*, Vol. 1, edited by N. G. Adams and L. M. Babcock (Greenwich, CT: JAI).
[20] Miller, D. R., 1988, *Atomic and Molecular Beam Methods*, edited by G. Scoles (Oxford University Press), p. 14.
[21] Mazely, T. L., and Smith, M. A., 1988, *J. chem. Phys.*, **89**, 2048.
[22] Toennies, J. P., and Winkelman, K., 1977, *J. chem. Phys.*, **66**, 3965.
[23] Randeniya, L. K., and Smith, M. A., 1990, *J. chem. Phys.*, **93**, 661.
[24] Mazely, T. L., Bristow, G. R., and Smith, M. A., 1995, *J. chem. Phys.*, **103**, 3688.
[25] Zacharias, H., Loy, M. M. T., Roland, P. A., and Sudbo, A. S., 1988, *J. chem. Phys.*, **81**, 3148.
[26] Belikov, A. E., Ahern, M. E., and Smith, M. A., 1997, *Chem. Phys.* (submitted).
[27] Dupeyrat, G., Marquette, J. B., and Rowe, B. R., 1985, *Phys. Fluids*, **28**, 1273.
[28] Wegener, P. O., 1959, *Phys. Fluids*, **2**, 264.
[29] Marte, J. E., Tschuikow Roux, E., and Ford, H. W., 1963, *J. chem. Phys.*, **39**, 3277.
[30] Baldacchini, G., Chakraborti, P. K., and D'Amato, F., 1992, *Appl. Phys.* B, **55**, 92.
[31] Abraham, O., Binn, J. H., DeBoer, B. G., and Stein, G. D., 1981, *Phys. Fluids*, **24**, 1981.
[32] Atkinson, D. B., and Smith, M. A., 1994, *J. chem. Phys.*, **98**, 5797.
[33] Ames Research Staff, 1975, National Advisory Committee for Aeronautics Report No. 1135.

[34] Daneshyar, H., 1976, *One Dimensional Compressible Flow* (Oxford: Pergamon).
[35] Adams, N. G., and Smith, D., 1983, *Reactions of Small Transient Species*, edited by A. A. Fontijn and M. A. A. Clyne, (New York: Academic Press), p. 311.
[36] Liu, S., Jarrold, M. F., and Bowers, M. T., 1985, *J. chem. Phys.*, **89**, 3127.
[37] Castleman, Jr, A. W., and Keesee, R. G., 1986, *Chem. Rev.*, **86**, 589.
[38] Chesnavich, W. J., and Bowers, M. T., 1977, *J. chem. Phys.*, **66**, 2306.
[39] Bates, D. R., 1980, *J. chem. Phys.*, **73**, 1000.
[40] Herbst, E., 1982, *Chem. Phys.* **68**, 323.
[41] Troe, J., 1977a, *J. chem. Phys.*, **66**, 4758; 1977b, *ibid.*, **66**, 4758; 1979, *J. chem. Phys.*, **83**, 114 (1979); 1987, *ibid.*, **87**, 2773.
[42] Light, J. C., 1967, *Discuss. Faraday Soc.*, **44**, 14.
[43] Bates, D. R., and Herbst, E., 1988, *Rate Coefficients in Astrochemistry*, edited by T. J. Millar and D. A. Williams (Dordrecht: Kluwer), p. 17.
[44] Herbst, E., and Bates, D. R., 1988, *Astrophys. J.*, **329**, 410.
[45] Smith, I. W. M., 1989, *Astrophys. J.*, **347**, 282.
[46] Gerlich, D., and Horning, S., 1992, *chem. Rev.*, **92**, 1509.
[47] Böhringer, H., and Arnold, F. A., 1982, *J. chem. Phys.*, **77**, 5534.
[48] Böhringer, H., Arnold, F., Smith, D., and Adams, N. G., 1983, *Int. J. Mass Spectrom. Ion Phys.*, **52**, 25.
[49] Ferguson, E. E., 1983, *Chem. Phys. Lett.*, **101**, 141.
[50] Randeniya, A. H. L. K., Zeng, X. K., and Smith, M. A., 1988, *Chem. Phys. Lett.*, **147**, 347.
[51] Randeniya, L. K., Zeng, X., and Smith, M. A., 1989, *J. chem. Phys.*, **93**, 8031.
[52] Hawley, M., and Smith, M. A., 1992, *J. chem. Phys.*, **96**, 1121.
[53] Randeniya, L. K., and Smith, M. A., 1990, *J. phys. Chem.*, **94**, 5205.
[54] Hawley, M., and Smith, M. A., 1992, *J. chem. Phys.*, **96**, 326.
[55] Barlow, S. E., Dunn, G. H., and Schauer, M. M., 1984, *Phys. Rev. Lett.*, **52**, 902.
[56] Barlow, S. E., Dunn, G. H., and Schauer, M. M., 1984, *Phys. Rev. Lett.*, **52**, 1610.
[57] Nakamura, H., 1992, *State Selected and State to State Ion Molecule Reaction Dynamics*, Part 2, edited by M. Baer and C. Y. Ng (New York: Wiley), pp. 243–320.
[58] Lindinger, W., Fehsenfeld, F. C., Schmeltekopf, A. L., and Ferguson, E. E., 1974, *J. geophys. Res.*, **79**, 4753.
[59] Gaucherel, P., Marquette, J. B., Rebrion, C., Poissant, G., Dupeyrat, G., and Rowe, B. R., 1986, *Chem. Phys. Lett.*, **132**, 63.
[60] Randeniya, L. K., and Smith, M. A., 1991, *J. chem. Phys.*, **94**, 351.
[61] Gerlich, D., and Kalmbach, H., 1990, Proceedings of the Third 'ECAMP, Bordeaux, 1990.
[62] Hawley, M., and Smith, M. A., 1997, *J. Phys. Chem.*, **96**, 6693.
[63] Sizun, M., and Kuntz, P. J., 1985, Proceedings of the Second 'ECAMP, Amsterdam, 1985, edited by A. E. DeVries and M. J. Van der Weil.
[64] Ferguson, E. E., 1983, *Chem. Phys. Lett.*, **99**, 89.
[65] Böhringer, H., Durum Ferguson, M., Ferguson, E. E., and Fahey, D. W., 1983, *Planet. Space Sci.*, **31**, 483.
[66] Böhringer, H., Durum Ferguson, M., Fahey, D. W., Fehsenfeld, F. C., and Ferguson, E. E., 1983, *J. chem. Phys.*, **79**, 4201.
[67] Dobler, W., Federer, W., Howorka, F., Lindinger, W., Durum Ferguson, M., and Ferguson, E. E., 1983, *J. chem. Phys.*, **79**, 1543.
[68] Kemper, P. R., and Bowers, M. T., 1984, *J. chem. Phys.*, **81**, 2634.
[69] Federer, W., Dobler, W., Howorka, F., Lindinger, W., and Durum Ferguson, M., 1985, *J. chem. Phys.*, **83**, 1032.
[70] Ferguson, E. E., 1986, *J. phys. Chem.*, **90**, 731.
[71] Kriegel, M., Richter, R., Tosi, P., Federer, W., Lindinger, W., and Ferguson, E. E., 1986, *chem. Phys. Lett.*, **124**, 583.
[72] Kriegel, M., Richter, R., Lindinger, W., Barbier, L., and Ferguson, E. E., 1988, *J. chem. Phys.*, **88**, 213.
[73] Tichy, M., Javahery, G., Twiddy, N. D., and Ferguson, E. E., 1988, *Chem. Phys. Lett.*, **144**, 131.

[74] MORRIS, R. A., VIGGIANO, A. A., DALE, F., and PAULSON, J. F., 1988, *J. chem. Phys.*, **88**, 4772.
[75] RICHTER, R., LINDINGER, W., and FERGUSON, E. E., 1988, *J. chem. Phys.*, **89**, 5692.
[76] LANDAU, L. D., and TELLER, E., 1936, *Phys. Z. Sowjetunion*, **10**, 34.
[77] LAMBERT, J. D., 1977, *Vibrational and Rotational Relaxation in Gases* (Oxford University Press).
[78] SCHELLING, F. J., and CASTLEMAN, A. W., 1984, *Chem. Phys. Lett.*, **11**, 47.
[79] HAWLEY, M., and SMITH, M. A., 1992, *J. chem. Phys.*, **95**, 8622.
[80] EBATA, T., and ZARE, R. N., 1986, *Chem. Phys. Lett.*, **130**, 467.
[81] KUO, C. H., BEGGS, C. G., KEMPER, P. R., BOWERS, M. T., LEAHY, D. J., and ZARE, R. N., 1989, *Chem. Phys. Lett.*, **163**, 291.
[82] TOSI, P., RONCHETTI, M., and LAGANA, A., 1987, *Chem. Phys. Lett.*, **138**, 495.
[83] TOSI, P., RONCHETTI, M., and LAGANA, A., 1988, *J. chem. Phys.*, **88**, 4814.
[84] ADAMS, N. G., SMITH, D., and ALGE, E., 1980, *J. Phys.* B, **13**, 3235.
[85] LINDINGER, W., 1986, *Int. J. Mass Spectrom. Ion Processes*, **70**, 213.
[86] LATIMER, D. R., and SMITH, M. A., 1994, *J. chem. Phys.*, **101**, 3852.
[87] LATIMER, D. R., and SMITH, M. A., 1994, *J. chem. Phys.*, **101**, 3410; 1994, Erratum, *ibid.*, **101**, 10197.
[88] MACKAY, G. I., SCHIFF, H. I., and BOHME, D. K., 1992, *Int. J. Mass Spectrom. Ion Processes*, **117**, 387.
[89] PRATT, S. T., DEHMER, P. M., and DEHMER, J. L., 1984, *Chem. Phys. Lett.*, **105**, 28.
[90] BECKER, H., HRUSAK, J., SCHWARZ, H., and BOHME, D. K., 1994, *J. chem. Phys.*, **100**, 1759.
[91] TICHY, M., JAVAHERY, G., TWIDDY, N. D., and FERGUSON, E. E., 1987, *Int. J. Mass Spectrom. Ion Processes*, **79**, 231.
[92] ADAMS, N. G., SMITH, D., TICHY, M., JAVAHERY, G., TWIDDY, N. D., and FERGUSON, E. E., 1989, *J. chem. Phys.*, **91**, 4037.
[93] CRUTZEN, P. J., 1970, *Q. Jl R. meterol. Soc.*, **96**, 320.
[94] JOHNSON, H. S., 1971, *Science*, **173**, 517.
[95] MCCONNELL, J. C., and MCELRON, M. B., 1973, *J. atmos. Sci.*, **30**, 1465.
[96] ANASTASI, C., and SMITH, I. W. M., 1978, *J. chem. Soc., Faraday Trans. II*, **74**, 1056.
[97] BURROWS, J. P., WALLINGTON, T. J., and WAYNE, R. P., 1983, *J. chem. Soc., Faraday Trans. II*, **79**, 111.
[98] DEMORE, W. B., SANDER, S. P., GOLDEN, D. M., MOLINA, M. J., HAMPSON, R. F., KURYLO, M. J., HOWARD, C. J., and RAVISHANKARA, A. R., 1990, *Chemical Kinetics and Photochemical Data for Use in Stratospheric Modeling, Evaluation Number 9*, Jet Propulsion Laboratory Publication No. 90, p. 1.
[99] ZABARNICK, S., 1993, *Chem. Phys.*, **171**, 265.
[100] TSANG, W., and HERRON, J. T., 1991, *J. Phys. Chem. Ref. Data*, **20**, 609.
[101] WAYNE, R. P., 1993, *Chemistry of Atmospheres*, second edition (Oxford University Press), p. 165.
[102] RAVASHANKARA, A. R., WINE, P. H., and LANGFORD, A. O., 1979, *Chem. Phys. Lett.*, **63**, 479.
[103] RAVISHANKARA, A. R., WINE, P. H., and WELLS, J. R., 1985, *J. chem. Phys.*, **83**, 447.
[104] CANNON, B. D., ROBERTSHAW, J. S., SMITH, I. W. M., and WILLIAMS, M. D., 1984, *Chem. Phys. Lett.*, **105**, 380.
[105] JOURDAIN, J. L., LE BRAS, G., and COMBOURIEU, J., 1981, *Chem. Phys. Lett.*, **78**, 483.
[106] CLARY, D. C., NYMAN, G., and HERNANDEZ, R., 1994, *J. chem. Phys.*, **101**, 3704.
[107] CLARY, D. C., NYMAN, G., and HERNANDEZ, R., 1993, *J. chem. Soc., Faraday Trans.*, **89**, 2185.
[108] CLARY, D. C., 1991, *J. chem. Phys.*, **95**, 7298.